Indian Journal of Chemistry
Vol. 65, May 2026, pp. 445-452
DOI: 10.56042/ijc.v65i5.22508

Synthesis, characterization, DFT studies, molecular docking and *in vitro* anti-bacterial activity of pyrazolone *p*-flurophenylhydrazone and its copper and manganese complexes

Chintan P Somaiya*[a], Ronak G Trivedi[a], Sushil N Pandey[a], Srujal A Sonera[a] & Shantaben K Kangad[b]

[a] Department of Chemical Science, Parul Institute of Applied Sciences, Parul University, Vadodara 391 760, Gujarat, India
[b] Department of Chemistry, Kamani Science College and Prataprai Arts College, Amreli 365 601, Gujarat, India
E-mail: somaiyachintan11@gmail.com

Received 7 August 2025; accepted (revised) 9 April 2026

This research focuses on the synthesis, characterization, computational studies and *in vitro* antibacterial studies of pyrazolone phenylhydrazone and its transition metal complexes of copper and manganese. Pyrazolone *p*-Flurophenylhydrazone has been synthesized and characterized using FT-IR, ^{1}H NMR and mass spectrometry. In the same way pyrazolone Cu (II) and Mn (II) transition metal complexes have been synthesized and characterized using FT-IR, ESI mass spectrometry, UV-Visible spectrometry and powder X-ray diffraction (XRD). In addition to these, Quantum mechanical Density Functional Theorycalculations have been simulated for ligand and metal complexes in order to obtain the electronic and structural properties and reactivity of the molecules. Furthermore, molecular docking studies have been carried out on Cu and Mn metal complexes with *E. coli* zinc deformylase inhibitor protein to access the interaction and binding of molecule with respect to the target site of receptor and compared with standard drugs Penicillin-G and Ampicillin. The antibacterial efficiency of ligand and its metal complexes have been evaluated against Gram-Positive and Gram-Negative bacterial assays to investigate its antimicrobial potential. These findings aid in the discovery of new successful leads with potential antimicrobial properties that can be optimized in future to get an effective drug candidates.

Keywords: 4-Acylpyrazolone, *p*-Flurophenylhydrazine, Computational chemistry, Density Functional Theory, Molecular docking, *in vitro* antimicrobial assay

Pyrazolones represent a significant class of heterocyclic compounds[3,5] characterized by the presence of nitrogen atoms at adjacent positions within the ring system and a ketone functional group at the 5th position[25,26]. In recent years, extensive research has been conducted on Schiff bases and their transition metal complexes, utilizing pyrazolone derivatives as key precursors. The synthesis of pyrazolone-based Schiff base[43] ligands typically involves a condensation reaction between 4-acyl pyrazolone[6,21] and phenyl hydrazine[4] derivatives leading to imine bond formation between carbon and nitrogen, accompanied by the elimination of water molecules. These Schiff base ligands exhibit diverse pharmacological[28] activities, including antimicrobial[9,34,,23], antifungal, antibacterial[1,38,29] anti-inflammatory[8,15], anticancer[8,10,15], antiviral[12], and antioxidant[7] properties. Schiff base ligands are having good chelating property with the transition metals, out of which mono and diamino derivatives of β-diketones are known for their chelating behavior. The coordination of respected pyrazolone phenyl hydrazone[14,15,18] electron donor ligands with transition metals enhances its biological activities.

In early research, complexation of Pyrazolone Schiff base ligands with transition metals greatly enhanced its biological potential as it allows easy penetration into the bacterial cell walls[27] and slow down the synthesis of Nucleic acids, proteins and amino[39] acids that leads to cell lysis and microbial death proving it a good antibiotic drug[35]; For example, Copper (II) Phenyl Butazone[42]. Pyrazolone Transition Metal complexes exhibit anti-cancer[7,22] properties by inducing processes such as cell cycle arrest, apoptosis and autophagy, ultimately resulting in cell death[43]. 4-Amino anti pyrine derivatives involving pyrazole moiety are effective against MCF-7 Human Breast Cancer and Caco-2 cancer cell lines. It is also effective against A-549 Human Lungs Cancer lines[10]. One of the complexes formed by reaction of phenylhydrazine and dinitrophenyl hydrazine with 4 Acetyl or 4-Benzoyl pyrazole that on coordination

with Cu (II) salt generates Cu (II) complex that are having good antioxidant activity and has the ability to penetrate the cancer[11] cells[45]. A recently designed and synthesized pyrazole derivatives are effective as potential inhibitors[30] of SARS-CoV-2[8] Main Protease (MPRO) possessing anti-viral property which has been identified using virtual screening technique[44].

Experimental Section

Materials

1-Phenyl-3-methyl-5-pyrazolone, *p*-fluorophenyl hydrazine, $CuSO_4 \cdot 6H_2O$, and $MnCl_2 \cdot 4H_2O$ were purchased from Sigma Aldrich. 1,4-Dioxane and methanol were purchased from Renkem.

Method

General procedure for Schiff base (L1)

The Schiff base (Fig. 1) was prepared in two step reaction in which in the first step about 10gm of respective pyrazolone was added in 25 ML 1,4-Dioxane in a round bottom flask and the RBF was placed on magnetic stirrer and stirred until it gets dissolved in solvent. After that Calcium Hydroxide was added in 1:2 mmol $Ca(OH)_2$ into RBF pinch wise with constant stirring. After that Butyryl chloride in 1:1 ratio was added into the above Ca complex with constant stirring and then whole system was placed in an oil bath and refluxed for 4 hrs at a temperature of 60-70°C. The progression of reaction was monitored through TLC. The orange to brown Acyl pyrazolone was obtained which was filtered and dried. In the second step of reaction, the above Acylated product was taken in a RBF and 4- Fluro[12] phenyl hydrazine[13] in equimolar concentration in different RBF. Acylated product was dissolved in 20 mL Methanol and 4-FPH was stirred with 20 mL of distilled water and then 20 mL of Methanol was added in it after half an hour. After both the material get completely dissolved, contents of both the RBF was combined, placed on magnetic stirrer on water bath and refluxed for 4-5 hours at a temperature of 60-70 °C. The progression of reaction was monitored through TLC. Upon conformation of reaction completion by TLC, the reaction mixture was cooled at RT and filtered.

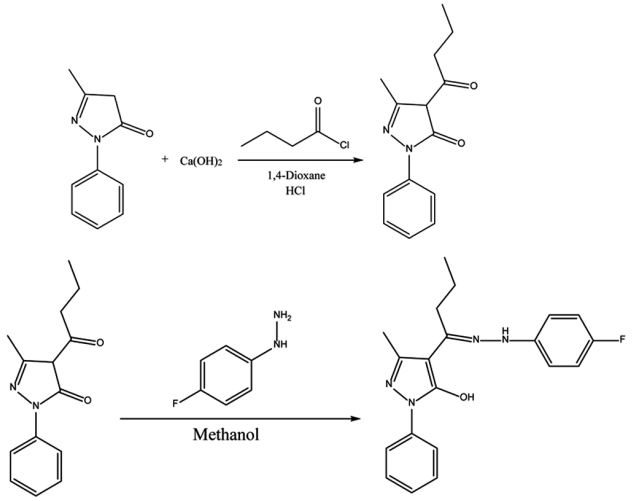

Fig. 1 — Synthesis of 4-flurophenylhydrazone ligand

L1: Mol. Formula $C_{20}H_{21}FN_4O$. m.p.325°C. Yield 88%. Yellow. FT-IR (KBr): 3061 (Ar.CH Str.), 1591 (C=N), 1624 (C=O), 3221 cm^{-1} (NH); 1H NMR (400 MHz, DMSO-d_6): δ 6.8 – 8.00 (Ar – H),12.4 (-OH), 6.2 (-NH), 1.00-2.4 (-CH_3); MS: *m/z* 352.17. Anal. C, 8.16; H, 6.01; N, 15.90; O, 4.54; F, 5.39%.

General procedure for Cu(II) and Mn(II) complex synthesis

Pyrazolone[24] Cu(II)[42] and Mn(II)[16,19,20] complexes (Fig. 2) were prepared by reacting ligand and metal salt in 2:1 reacting ratio. For that calculated amount of pyrazolone phenyl hydrazone Schiff base ligand was taken in an RBF and 10 mL of methanol was added into it. This reaction mixture was refluxed on water bath for half an hour. After that alkaline methanolic solution was prepared by adding 2-3 mL of distilled water and 5 mL of methanol which was added into the refluxing medium. Now calculated amount of metal

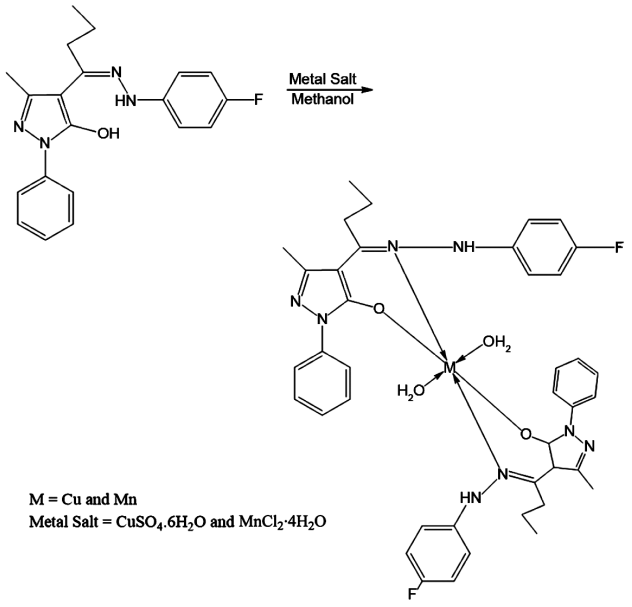

Fig. 2 — Synthesis of Cu (II) and Mn(II) Metal complexes (CuL1 and MnL1)

salt ($CuSO_4.6H_2O$ or $MnCl_2.4H_2O$) was accurately weighed and taken into a small beaker. 5 mL of distilled water was added to dissolve the metal salt and then 10 mL of methanol was added into it. This metal salt solution was added dropwise into the refluxing mixture for complexation process and refluxed for 4-5 hours. Reaction completion was examined using TLC. Upon confirmation of product spot on TLC, the reaction mass was cooled and transferred into a 250 mL beaker. This reaction mixture was placed in to fumehood and solvent was allowed to evaporate. After evaporation, reaction mixture was filtered, washed and dried to obtain pure solid of Cu (II) or Mn (II) complexes of pyrazolone Schiff base ligand.

CuL1: Mol. Formula $C_{40}H_{44}CuF_2N_8O_4$. m.p. >300°C. Yield 76%. Greyish Green. FT-IR (KBr): 3065.99 (-OH stretch), 2963.98 (Ar -CH stretch), 691.42 (Cu-O stretch), 612.88 (Cu-N stretch), 1220.93 (C-N stretch), 1702.93 cm^{-1} (-CO stretch); MS: *m/z* 852.01. Anal. C, 59.88; H, 5.53; Cu, 7.92; F, 4.74; N, 13.97; O, 7.98%.

MnL1: Mol. Formula $C_{40}H_{42}MnClF_2N_8O_3$. m.p. >300°C. Yield 80%. Grey. FT-IR (KBr): 2961.11 (Ar.CH Str.), 1153.74 (C=N), 1594 (C=O), 609.29 (M-O stretch), 673.80 (M-Cl stretch), 755.55 cm^{-1} (M-N stretch); MS: *m/z* 810.24.

Result and Discussion

^{1}H NMR analysis, L1

Pyrazolone 4-flurophenylhydrazone Schiff base and its metal complexes is known for its dynamic keto enol tautomerism. The ^{1}H NMR data of synthesized pyrazolone 4-Fluorophenylhydrazone ligand is carried out in DMSO d6 solvent at RT all the obtained data is represented in experimental section, in the case of 1H NMR spectra of ligand peak obtained near to 12.4 ppm correspond to the -OH group, aromatic proton in L1 are observed in range of 6.7-7.2 ppm, triplet of methyl group is observed in the range of 1.05 ppm and sextet of methylene protons observed in the range of 1.6 to 2.4 in L1. All the data supports the structure of synthesized ligand. Based on these data it is observed that ligand exist in keto enol form in solution state.

Infrared Spectra

The IR spectra of ligand L1 and their Cu (II) and Mn (II) metal complex provides detailed information about the nature of functional groups attached to metal ion. In the IR spectra of ligand(L1) a sharp peak is observed in the range of 1591 cm^{-1} corresponding to the acyclic azo methine group. In the complexes where the ligand coordinated to the metal ion through the Nitrogen atom a reduction in electron density in a azomethine link is expected resulted in the appearances of a peak at 1220 cm^{-1}. The IR spectrum of ligand exhibit prominent band in the range 1591-1624 cm^{-1} attributed to the stretching mode of carbonyl group upon complexation these band disappears and the new band emerges at 1702 cm^{-1} suggesting the involvement of oxygen atom in the complex formation. Furthermore, the proposed coordination sites are supported by medium band observed between 612 cm^{-1} and 691 cm^{-1} which can be attributed to M-N and M-O modes respectively. Based on the above discussion it can concluded that the coupling process between ligand and metal ion leads to the formation of complexation.

Mass Spectral Studies (Ligand)

In the mass spectra of Ligand (L1), Molecular ion peak and base peak was observed at m/z 352 which was the most intense and stable peak in spectra corresponding to the theoretical molecular weight of the molecule which is about 352.17 gm/mol.

Mass Spectral Studies (Complex)

The mass spectral (ESI mass) (Fig. 3) study of metal complex **CuL1** has been carried out. The sharp peak observed at m/z =852.29 represent molecular ion peak and base peak observed at m/z=758.15 which is coincident with the formula weight of the metal complex.

Powder X-Ray Diffraction Analysis

X-ray powder diffraction (XRD) is a rapid analytical technique primarily used for phase

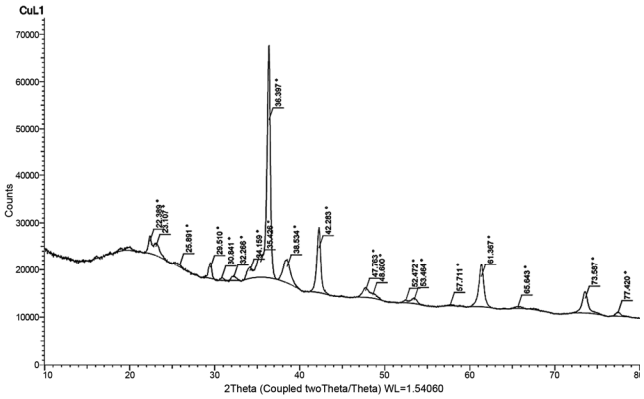

Fig. 3 — ESI Mass and X-Ray diffraction peak of CuL1

identification of a crystalline material and can provide information on unit cell dimensions.

X-ray diffraction is based on constructive interference of monochromatic X-rays and a crystalline sample. These X-rays are generated by a cathode ray tube, filtered to produce monochromatic radiation, collimated to concentrate, and directed toward the sample. The interaction of the incident rays with the sample produces constructive interference (and a diffracted ray) when conditions satisfy Bragg's Law ($n\lambda=2d \sin\theta$).

Powdered X-Ray Diffraction studies were carried out on Copper metal complex (Fig. 3) to study its crystalline nature and interplanar spacing with the help of 2θ value determined from curve.

The diffractogram of Copper (II) complex shows 20 reflections with maxima at 2θ= 36.397°. The observed unit cell parameters are a = 4.686 Å, b = 3.4250 Å, c = 5.1320 Å and α = 90°, β = 99.42° and γ = 90°. The complex satisfies the condition a ≠ b ≠ c and α = γ = 90° and β ≠ 90° and therefore the compound is monoclinic.

UV-Visible Spectra

The intense band at ~270 nm corresponds to ligand-centered π → π* or n → π* transitions, indicative of aromatic ligands like Schiff bases. A broader absorption in the visible region (~500~700 nm) is attributed to d-d transitions of the central metal ions. For Cu^{+2}, the band near 600-700 nm arises due the $^2E_g \rightarrow {}^2T_{2g}$ transitions in a distorted octahedral geometry. For Mn^{+2} weak absorptions occur due spin-forbidden d-d transitions typically between 400-500nm.

Computational Study

Density Functional Theory (DFT) [2,17,40,41] are used to elucidate electronic states of atoms and molecules by optimizing the structures through mathematical quantum mechanical calculations. DFT calculations was conducted for both the Copper and Manganese Complexes. All the calculations were performed utilizing the B3LYP / LANL2DZ basis set with +2 charge and doublet spin.

Geometry Optimization

The initial 3D structures of the synthesized compounds were prepared using GaussView 6.0, with calculation parameters configured for employing the B3LYP/LANL2DZ basis set. Gaussian 9.0W interface was utilized for calculations. The optimized three-dimensional atomic structure was visualized through Gauss view 6.0. (Fig. 4)

FMO

A concept in organic chemistry known as frontier molecular orbital (FMO) theory aids in the prediction and explanation of the stability, selectivity, and reactivity of organic compounds. The theory focusses on a molecule's Frontier Orbitals, which are its lowest unoccupied molecular orbital (LUMO) and highest occupied molecular orbital (HOMO). A molecule's ability to donate electrons is represented by its HOMO, and its ability to accept electrons is represented by its LUMO. In chemical reactions, a molecule's interaction with another molecule is determined by the relative energies and spatial distribution of these orbitals. For the compounds with the same names, the HOMO and LUMO energies and their associated band gap were calculated using Density Functional Theory (DFT) simulations using the B3LYP function and the LANL2DZ basis set.

The HOMO of a molecule, which indicate its capacity to donate electron is usually represented by the

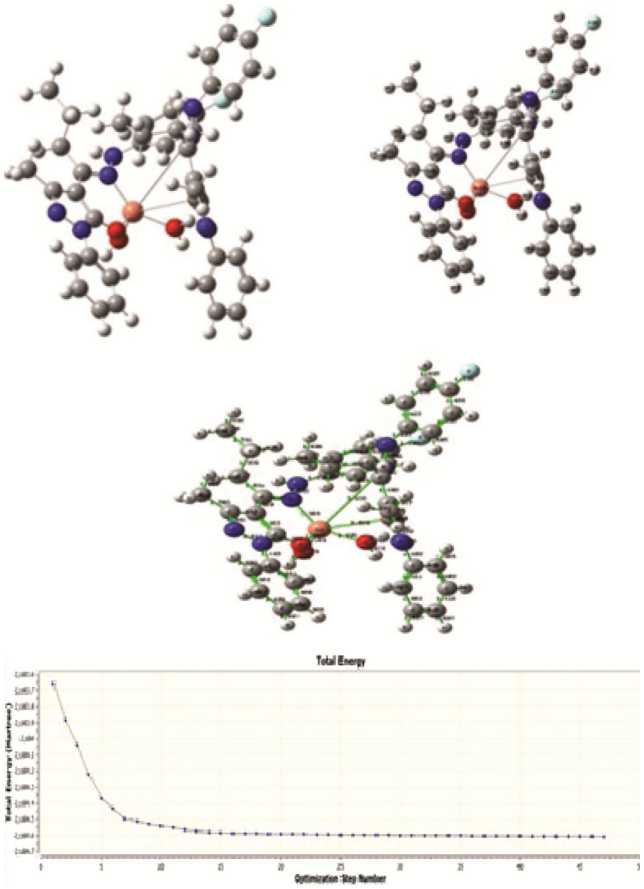

Fig. 4 — optimisation result of CuL1

red colour of a HOMO-LUMO energy map. The molecule's ability to accept electron is indicated by the green portion which stands for Lowest Unoccupied Molecular Orbital (LUMO). The reactivity of the molecule is determined by the energy gap between these orbitals, a smaller gap denotes higher reactivity. The stability of the ligand is indicated by negative values for E_{HOMO} and E_{LUMO} in the molecule energy level diagram. This implies that the molecule has a favourable electronic structure, which is advantageous in a variety of chemical applications. Important molecule characteristics like the energy[36] gap, ionisation potential, electronegativity, electron affinity, chemical hardness, softness, and electrophilicity index are all determined by the HOMO and LUMO energies.

Electronic Parameters

Some of the electronic parameters are:

(1) Energy gap (ΔE) = $E_{LUMO} - E_{HOMO}$, (2) Ionization potential (IP) = $-E_{HOMO}$, (3) Chemical potential (μ) = ½ ($E_{HOMO} + E_{LUMO}$), (4) Electron affinity (EA) = $-E_{LUMO}$, (5) Electron Negativity (EN) = –½ ($E_{HOMO} + E_{LUMO}$), (6) Global Hardness (η) = –½ ($E_{HOMO} - E_{LUMO}$),

(7) Softness (S) = $1/2\eta$, (8) Electrophilicity Index (ω) = $\mu^2/2\eta$.

The electronic parameters are shown in Table 1.

MEP-Surface

MEP is an important concept in computational chemistry to get information about electric charge distribution within the molecule. MEP is visualized as a color map, region with high electron density is depicted in orange or red region, which indicate area where positively charged species would be attracted, while the region with low electron density depicted in blue color indicating area of repulsion while the area in green portion represents the neutral potential.

Table 1 — Electronic Parameters

c	Properties	CuL1	MnL1
1	Total Energy (K eV)	–73051.9018	–68862.5710
2.	E_{HOMO} (eV)	–10.212	–10.757
3.	E_{LUMO} (eV)	–9.709	–10.409
4.	ΔE (eV)	0.503	0.348
5.	Ionization potential (IP) (eV)	10.212	10.757
6.	Chemical potential (μ) (eV)	–9.9605	–10.583
7.	Electron affinity (EA) (eV)	9.709	10.409
8.	Electron Negativity (EN) (eV)	9.9605	10.583
9.	Global Hardness (η) (eV)	0.2515	0.174
10.	Softness (S) (eV^{-1})	0.1257	0.087
11.	Electrophilicity Index (ω) (eV)	197.2395	321.836
12.	Dipole Moment (Debye)	4.0592	55.5371

2D Fingerprint region and Hirshfeld Surface Area Analysis

2D fingerprint plot is a visual representation of intermolecular interactions in the crystal structure of the molecules. It maps the distance from a point on the molecular surface to the nearest atom in the same molecule (d_i) and the nearest atom in the neighboring molecule (d_e).

Peaks and regions indicate specific interactions like H-H, C-H, O-H, C-N and so on.

Hirshfeld surface area analysis visualizes the 3D molecular surface and highlights where the interaction occurs. The surface is defined by the region where the electron density of a molecule becomes equal to the surrounding environment.

d_{norm} shows color coded maps where red color indicates close contacts, blue color indicates longer distances and white color indicates neutral contacts.

Shape Index shows complementary surfaces for π-π stacking interactions and curvedness describes how flat or curved the surface is which indicates planar stacking or molecular shape (Table 2).

Molecular Docking

Molecular docking[10,44] is a computational technique used to study the affinity of small molecule(ligand) with a target receptors or macromolecules (Usually a Protein[37]). The goal is to study the interaction of ligand with a receptor and to identify the potential drug candidates.

The Molecular docking utilized a combination of certain computational tools like AutoDock, Molecular Operating Environment (MOE), Biovia Discovery Studio visualizer for preparation of input files, to minimize ligand energy and visualization and analysis of docking results.

In this research molecular docking study was undertaken to evaluate synthesized compound against antimicrobial *E. coli zinc deformylase inhibitor complex protein* (PDB Id; 1BSK). Furthermore, penicillin and ampicillin (Fig. 5)were subjected to molecular docking against the same macromolecule in

Table 2 — Interatomic interaction within the molecule

	Percentage Interaction between atoms (%)				
Atoms	All	Carbon	Fluorine	Nitrogen	Oxygen
All	99.9	74.7	21.6	3.7	0.0
Carbon	78.5	53.4	21.6	3.6	0.0
Fluorine	10.9	10.9	0.0	0.0	0.0
Nitrogen	5.1	5.1	0.0	0.0	0.0
Oxygen	1.7	1.7	0.0	0.0	0.0

order to get effective comparison antimicrobial efficacy between standard and synthesized molecules (Table 3 and Table 4).

Both the Penicillin G and Ampicillin was docked with the said protein to characterize its antimicrobial efficacy, 2D and 3D interaction and other useful parameters.

RMSD (Root Mean Square Deviation) and Binding Energy should be less in order to have efficient and effective binding of molecules into the active site of the receptor.

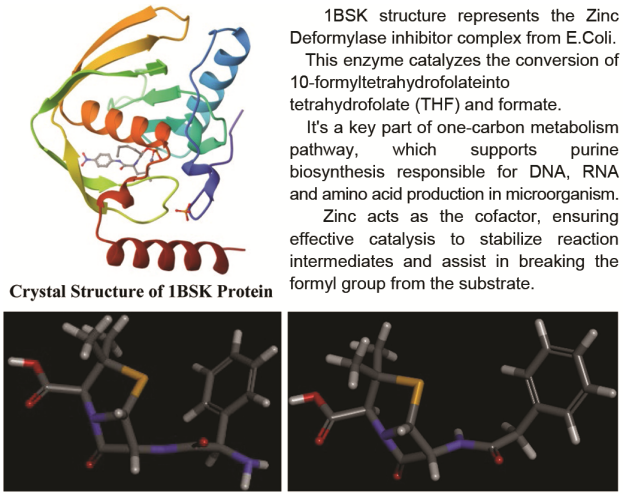

Fig. 5 — 3D structure of Penicillin-G and Ampicillin

RMSD Values should be less than or equal to 2 and docking score should be less.

By comparing the docking results of standard drugs with synthesized metal complexes, we found that Copper (II) Complex (Fig. 6) is showing RMSD and binding scores approximately correlating with that of standard drugs[31,32,37]. Therefore, it should be having good binding with anti-microbial protein and it may show good antimicrobial activity which was then examined by *in vitro* antimicrobial testing on Gram-Positive and Gram-Negative bacteria.

Here, Manganese (II) complex is highly deviating from standard value. Therefore, it may show less binding[33] and also less anti-microbial activity against microbes.

Table 3 — Docking results of standard drugs with anti-microbial *E. coli*

Standard Drugs	Docking score	RMSD Values	Binding Energy
Penicillin-G	–6.0637	1.4945	–6.0637 kcal/mol
Ampicillin	–6.3063	1.4609	–6.3063 kcal/mol

Table 4 — Docking result of copper and manganese metal complexes with antimicrobial *E. coli* protein

Metal Complexes	Binding Score	RMSD Values	Binding Energy
Copper (II) Complex	–5.6392	1.2658	–5.6392 kcal/mol
Manganese (II) Complex	–5.5166	2.4531	–5.5166 kcal/mol

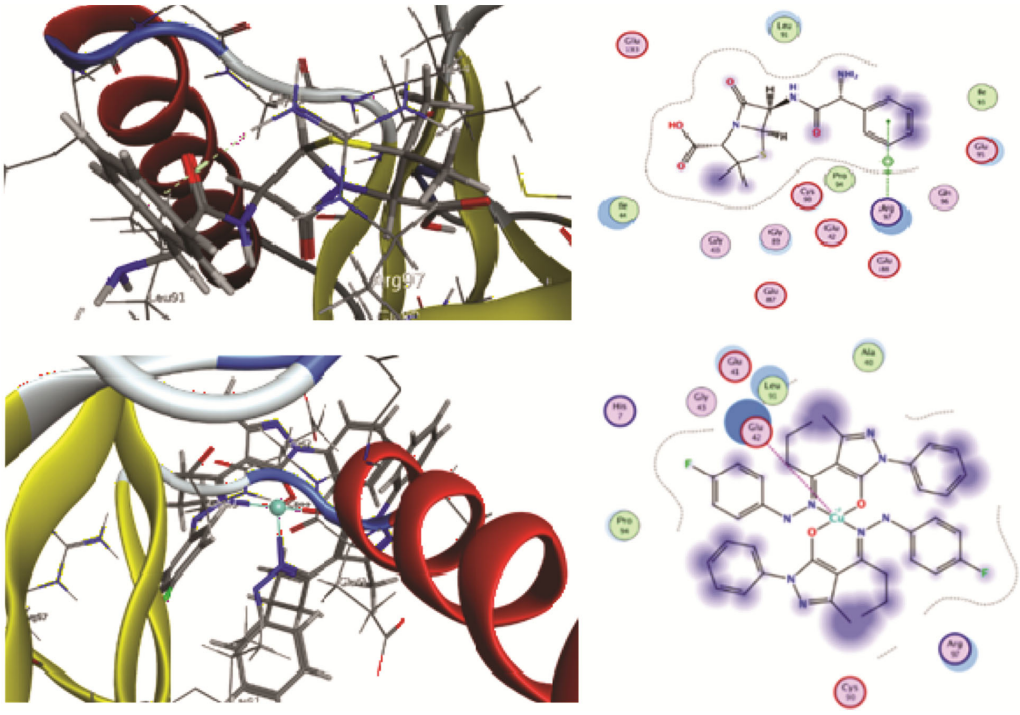

Fig. 6 — 2D and 3D interaction of CuL1 with protein

Table 5 — Zone of Inhibition(mm) of the Schiff-Base compounds against Gram-positive and Gram-negative bacteria

S. No.	Compd	Gram-positive (*Staphylococcus aureus*)	Gram-negative (*Escherichia coli*)
1	Penicillin	30	20
2	Ampicillin	24	19
3	L1	18	11
4	CuL1	21	16
5	MnL1	19	15

Antimicrobial Activity

This study asses the antimicrobial efficacy of the synthesized compound against Gram – Positive *(Staphylococcus aureus)* and Gram- Negative *(Escherichia coli)* bacteria using the agar gel diffusion method. Gram-positive bacteria have single thick layer of peptidoglycan in their cell wall while Gram-negative bacteria have thin layer peptidoglycan surrounded by an outer membrane. Penicillin and Ampicillin served as a reference drug. The result obtained are mentioned in Table 5.

Conclusion

This research highlights the synthesis of Pyrazolone 4-Flurophenylhydrazone Schiff bases and its transition metal complexes (Copper and Manganese) using corresponding metal salts. Characterization of the synthesized ligand and msetal complexes were carried out using various spectroscopic techniques such as Mass, FTIR, NMR, ESI Mass and UV-Visible Spectrometry. Computational modelling and analysis of electronic and structural parameters of the complexes were carried out using Density Functional Theory Calculations (DFT) on Gauss View interface using Gaussian 09W calculation tool. 2D Fingerprint region and Hirshfeld surface area analysis was done using Vesta and Crystal Explorer software tools.

Furthermore, molecular docking technique was used to identify the interaction of metal complexes with anti-microbial E. coli deformylase target protein in order to know the biological and pharmacological activity against microbes.

Additionally, *in vitro* antimicrobial screening was carried out using gram-positive and gram-negative bacteria to examine its effect against microbes by comparing the zone of inhibition values with the standard drugs *i.e.*, Penicillin-G and Ampicillin.

Supplementary Information

Supplementary information is available in the website https://nopr.niscpr.res.in/handle/123456789/58776.

References

1 Abera S, Dessalegn T & Endale M, *Chem Mat Res*, 10 (2018) 12.
2 Al-Janabi A S, Elzupir A O, Abou Krisha M M & Yousef T A, *Inorganics*, 11 (2023) 63.
3 Altalbawy F M A, *Asian J Chem*, 27 (2015). (https://doi.org/10.14233/ajchem.2015.19123).
4 Atanasković A, Eichhorn T, Milenkovic D, Dimić D, Kaluđerović G & Marković J D, *2nd International Conference on Chemo and Bioinformatics*, (2023). (https://doi.org/10.46793/ICCBI23.395A).
5 Azab M E, Rizk S A & Amr A E G E, *Molecules*, 20 (2015) 18201.
6 Bakanas I J & Moura L G, *Eur J Org Chem*, 2016 (2016) 5345. https://doi.org/10.1002/ejoc.201601093.
7 El Gammal O A, Abdel-Latif E, Fara M G & Abdel R M H, *App Organomet Chem*, 35 (2021) e6194.
8 Magda A A, Abdel Aziz N I, Alaa A M, El-Azab A S, Asiri Y A & ElTahir K E H, *Bioorg Med Chem*, 19 (2011) 3416.
9 Gabra N M, Samir B M, Zaki H A, Elhag M A & Babiker A H, *Int J Sci Res*, 6 (2015) 1794.
10 Ghabbour H A, Qabeel M M, Eldehna W M, Al Dhfyan A & Abdel-Aziz H A, *J Chemistry*, 2014 (2014) 154357. (https://doi.org/10.1155/2014/154357)
11 Ghorab M M, El Gazzar M G & Alsaid M S, *Int J Mole Sci*, 15 (2014) 7539.
12 Karad S C, Purohit V B & Raval D K, *Eur J Med Chem*, 84 (2014) 51.
13 Abebe H, Lamma T, Filkale A & Kure D, *Chem Rxiv* (Preprint), (2024). (https://doi.org/10.26434/chemrxiv-2024-d4cjt).
14 Lapasam A, Dkhar L, Joshi N, Poluri K M & Kollipara M R, Inorg Chimica Acta, 484 (2019) 255.
15 Mujafarkani N, Bassey V, Tokono J J, Ahamed A J, Benjamin I, Agurokpon D C & Louis H, *Heliyon*, 9 (2023) e18067. (https://doi.org/10.1016/j.heliyon.2023.e18067).
16 Ibrahim O B, Mohamed M A & Refat M S, *Can Chem Trans*, 2 (2014) 108.
17 Shakdofa M M, Morsy N A, Rasras A J, Al-Hakimi A N & Shakdofa A M, *App Organomet Chem*, 35 (2021) e6111.
18 Solankee A & Tailor R, *Int Lett Chem Phy Astro*, 47 (2015) 109.
19 Somaiya C P, Patel D S & Jani D H, *J Emerg Tech Innov Res*, 6 (2019) 247. (https://www.academia.edu/download/83766582/C.P_Somaiya_JETIR.pdf.)
20 Somaiya C P, Patel D S & Jani D H, *J App Chem*, 8 (2019) 1135.
21 Somaiya C P, Patel N M, Prajapati V P, Bhavsar S H, Shah J H & Shevale A D, *Eur Chem Bull*, 12 (2023) 3398. (http://dx.doi.org/10.48047/ecb/2023.12.7.280).
22 Noma S A A, Erzengin M, Tunç T & Balcıoğlu S, J Mol Struc, 1205 (2020) 127550.
23 Somaiya C P, Patel D S, Jani D H & Thanki D R, *Indian J Chem*, 63 (2024) 1015.
24 Somaiya C P, Yadav D A, Dadhaniya H R, Patel V J & Raulji J B, *Int J Bio Pharm Allied Sci*, 13 (2024) 5523.
25 Bellina F, Cauteruccio S & Rossi R, *Tetrahedron*, 63 (2007) 4571.
26 Mazel D, Pochet S & Marliere P, *EMBO J*, 13 (1994) 914.
27 Meinnel T, *Parasit Today*, 16 (2000) 165.
28 Whitworth J A, *J Hypertens*, 21 (2003) 1983.

29 Chen D Z, Patel D V, Hackbarth C J, Wang W, Dreyer G, Young D C, Margolis P S, Wu C, Ni Z-J, Trias J, White R J & Yuan Z, *Biochemistry*, 39 (2000) 1256.

30 Yoo J-S, Zheng C-J, Lee S, Kwak J-H, Kim W-G & Macrolactin N, *Bioorg Med Chem Lett*, 16(2006) 4889.

31 Walters W P & Namchuk M, *Nat Rev Drug Disc*, 2 (2003) 259.

32 Oprea T I, Davis A M, Teague S J & Leeson P D, *J Chem Inf Comp Sci*, 41 (2001) 1308.

33 Baell J B, *Int J Curr Res*, 4 (2012) 505.

34 Agarwal T, Singh A & Asthana S, *Int J Curr Res*, 4(2012) 505.

35 Agarwal T, Asthana S, Gupta P & Khursheed A, *Int J Pharm Pharm Sci*, 6 (2014) 379.

36 Morris GM, Goodsell DS, Halliday RS, Huey R, Hart WE, Belew R K & Olson A J, *J Comput Chem*.;19(199814):1639-62.

37 Laskowski R A & Swindells M B, *J Chem Inf Model*, 51(2011) 2778.

38 Verma SK, Jat R & Nagar N, *Pharmacophore J*, 2 (2011) 114.

39 Meinnel T, Blanquet S & Dardel F, *J Mol Biol*, 262 (1996) 375.

40 Manjuraj T, Yuvaraj T C M, Jayanna N D & Sarvajith M S, *Mat Today Proc*, 54 (2022), 646.

41 Mohan M, Pangannaya S, Satyanarayan M N & Trivedi D R, *Opt Mate*, 77 (2018) 211.

42 Suma S, Sudarsanakumar M R, Nair C G R & Prabhakaran C P, *Indian J Chem, Sect A*, 32 (1993) 67.

43 Presenjit, Chaturvedi S, Singh A, Gautam D, Singh K & Mishra A K, *Anti-Can Agents Med Chem*, 24 (2024) 488.

44 Rekharani D, Shivalingegowda N, Mahesha, Urs M V D, Chethan B S & Krishnappagowda L N, *Chem Phy Impact*, 8 (2024) 100475.

45 Verdicchio F, Pyrazolone-based metal complexes: synthesis, characterization and theoretical study of Zn (II), Cu (II) and Mo (IV) derivatives. (https://hdl.handle.net/20. 500. 14242/160588).